HHS Public Access

Author manuscript

Chem Biol. Author manuscript; available in PMC 2016 May 21.

Published in final edited form as:

Chem Biol. 2015 May 21; 22(5): 619–628. doi:10.1016/j.chembiol.2015.04.013.

Peroxide-dependent MGL sulfenylation regulates 2-AG-mediated endocannabinoid signaling in brain neurons

Emmanuel Y. Dotsey[1], **Kwang-Mook Jung**[2], **Abdul Basit**[3], **Don Wei**[2], **Jennifer Daglian**[2], **Federica Vacondio**[4], **Andrea Armirotti**[3], **Marco Mor**[4], and **Daniele Piomelli**[1,2,3,5,*]

[1]Department of Pharmacology, University of California, Irvine, Irvine, CA 92697

[2]Department of Anatomy and Neurobiology, University of California, Irvine, Irvine, CA 92697

[3]Drug Discovery and Development, Istituto Italiano di Tecnologia, 16163 Genoa, Italy

[4]Pharmaceutical Department, University of Parma, Parma 43100, Italy

[5]Department of Biological Chemistry, University of California, Irvine, Irvine, CA 92697

SUMMARY

The second messenger hydrogen peroxide transduces changes in cellular redox state by reversibly oxidizing protein cysteine residues to sulfenic acid. This signaling event regulates many cellular processes, but has been never shown to occur in the brain. Here we report that hydrogen peroxide heightens endocannabinoid signaling in brain neurons through sulfenylation of cysteines C201 and C208 in monoacylglycerol lipase (MGL), a serine hydrolase that deactivates the endocannabinoid 2-arachidonoyl-*sn*-glycerol (2-AG) in nerve terminals. The results suggest that MGL sulfenylation may provide a presynaptic control point for 2-AG-mediated endocannabinoid signaling.

INTRODUCTION

Activation of metabotropic glutamate receptor-5 ($mGluR_5$) in dendritic spines stimulates release of the lipid-derived endocannabinoid transmitter, 2-AG, which crosses the synapse in a retrograde direction to engage CB_1 cannabinoid receptors on axon terminals and suppress glutamate release (Castillo et al., 2012). This negative feedback mechanism is thought to modulate excitatory synaptic transmission throughout the central nervous system (CNS) (Katona and Freund, 2008). Along with $mGluR_5$, another checkpoint for endocannabinoid signaling may be provided by MGL, a presynaptic serine hydrolase that cleaves 2-AG into

*Corresponding Author: Dr. Daniele Piomelli, Department of Anatomy and Neurobiology, 3101 Gillespie NRF, University of California, Irvine, CA 92697-1275. Phone: (949) 824-6180 Fax: (949) 824-6305 piomelli@uci.edu.

AUTHOR CONTRIBUTIONS

E.Y.D. carried out MGL inhibition and cell viability experiments with help from D.W. and J.D.. A.B., K.-M.J. and A.A. performed MGL sulfenylation studies. E.Y.D, K.-M.J., A.A., F.V., M.M. and D.P. analyzed the data. M.M. and D.P. designed the project. D.P. coordinated the project and wrote the manuscript with help from E.Y.D, K.-M.J., A.A., and M.M..

arachidonic acid and glycerol, terminating its biological actions (Dinh et al., 2002; Gulyas et al, 2004). Genetic and pharmacological interventions that either enhance (Jung et al, 2012) or interrupt (Hohmann et al., 2005; Long et al, 2009) MGL activity are known to affect the pool of bioactive 2-AG, but whether posttranslational MGL modifications influence 2-AG signaling remains undetermined.

The catalytic site of MGL is partially covered by a flexible 'cap' domain that controls the entry of substrates into the enzyme's active site (Labar et al, 2010; Bertrand et al, 2010; Schalk-Hihi et al, 2011)(Figure 1A). This domain harbors two cysteine residues (C201 and C208) that mediate the interaction of MGL with thiol-reacting inhibitors such as benzisothiazolinones (King et al, 2009) and N-acyl-substituted maleimides (Saario et al, 2005). A third cysteine (C242) located within the active site, in close proximity of the catalytic nucleophile S122, directly influences catalysis (Labar et al, 2010; Saario et al, 2005). These residues might be targeted by the second messenger, hydrogen peroxide (H_2O_2), which modifies protein function (Patel and Rice, 2012) through reversible oxidation of cysteine's thiol groups (-SH) to sulfenic acid (-SOH) (Dickinson and Chang, 2011; Lo Conte and Carroll, 2013). Because ionotropic glutamate receptors stimulate H_2O_2 production (Patel and Rice, 2012) and H_2O_2 influences the activities of several functionally important neuronal proteins (Rice, 2011), we hypothesized that peroxide-dependent sulfenylation of the regulatory cysteines, C201 and C208, might inhibit MGL and, by doing so, heighten 2-AG-mediated endocannabinoid signaling. If confirmed experimentally, this mechanism would provide a presynaptic control point for 2-AG-mediated endocannabinoid signaling at central excitatory synapses.

RESULTS AND DISCUSSION

Hydrogen peroxide inhibits MGL

The flexible 'cap' domain of MGL, which contains the regulatory cysteines C201 and C208, controls the entry of substrates into the enzyme's active site (Labar et al, 2010; Bertrand et al, 2010; Schalk-Hihi et al, 2011) (Figure 1A). We hypothesized that peroxide-dependent sulfenylation of these two residues might inhibit MGL and thus heighten 2-AG-mediated signaling. As a first test of this idea, we exposed recombinant rat MGL to concentrations of H_2O_2 that are known to reversibly affect protein function without causing oxidative damage (Rice, 2011). H_2O_2 inhibited MGL with a median effective concentration (IC_{50}) of 8.2 ± 1.3 μM (Figure 1B). The inhibition was rapid (Figure 1C), displayed noncompetitive Michaelis-Menten kinetics (Figure 1D), and was fully reversible upon enzyme dilution (Figure 1E). By contrast, even at very high concentrations, H_2O_2 did not affect the activity of recombinant diacylglycerol lipase-α (DGL-α) (Figure 1B), the serine hydrolase that catalyzes $mGluR_5$-operated 2-AG formation in spines (Castillo et al., 2012; Katona and Freund, 2008).

Role of regulatory cysteines C201 and C208

We used site-directed mutagenesis to determine whether the three regulatory cysteine residues present in MGL – C201, C208 and C242 – contribute to peroxide-dependent enzyme inhibition. Replacing either C201 or C208 with alanine caused a rightward shift in the potency of H_2O_2 (Figure 1B and Table S1). Importantly, an even more pronounced shift

was observed when both C201 and C208 were mutated (Figure 1B and Table S1), which is suggestive of a cooperative interaction between the two residues. By contrast, replacing C242 with alanine or serine had no effect on H_2O_2-induced inhibition of MGL activity (Figure 1F). The inhibitory actions of H_2O_2 were also apparent when the oxidant was applied on intact mouse Neuro-2a cells. In these experiments, we used H_2O_2 at concentrations of 30-300 μM, in consideration of the fact that only 1-10% of externally applied H_2O_2 crosses the cell membrane (Rice, 2011). In native Neuro-2a cells, H_2O_2 inhibited MGL activity in a concentration-dependent manner (Figure S1A) and this effect was paralleled by an increase in intracellular 2-AG content (Figure S1B). In Neuro-2a cells that overexpressed the C201/C208 double mutant form of MGL, H_2O_2 only weakly inhibited MGL activity (Figure S1C) and did not increase 2-AG levels (Figure S1D). Together, these findings indicate that H_2O_2 inhibits MGL at concentrations similar to those demonstrated to be active on other biologically relevant targets, such as protein tyrosine phosphatase 1B (Denu and Tanner, 1998) and endothelial growth factor receptors (Paulsen, 2011). Inhibition occurs through an allosteric mechanism that involves the redox-sensitive cysteines C201 and C208, which respond cooperatively to H_2O_2-induced oxidation.

Hydrogen peroxide causes C201 and C208 sulfenylation

To determine whether MGL is a substrate for cysteine sulfenylation, we incubated the purified recombinant enzyme with H_2O_2 in the presence of dimedone – a chemoselective probe that reacts with short-lived sulfenyl groups in cysteines to form stable thioethers (Figure 2A, inset) (Pan and Carroll, 2014) – and then digested the protein with trypsin. Liquid chromatography/mass spectrometry (LC/MS) analyses of the tryptic digest showed that dimedone was exclusively bound to the peptides containing C201 (SEVDLYNSDPLIC<u></u>HAGVK) (Figure 2A,B) and C208 (VC<u></u>FGIQLLNAVSR) (Figure 2A,C). No other dimedone-bound peptides were observed (Figure S2). Further high-resolution LC/MS studies revealed that C201 was mainly present as thiol or sulfenic acid, although minor quantities (1-7%) of sulfinic ($-SO_2H$) and sulfonic ($-SO_3H$) acids were also detected (Figure 2D). C208 was less sensitive than C201 to oxidation and yielded approximately equal amounts of sulfenic, sulfinic and sulfonic acids (Figure 2E). Tandem MS analyses of the two dimedone-labeled tryptic fragments of MGL allowed us unequivocally to assign C201 and C208 as the sites of sulfenylation induced by H_2O_2 (Figures 3A,B). Lastly, using biotin-1,3-cyclopentanedione (BP1), a biotin-containing dimedone derivative that can be used for affinity precipitation (Qian et al, 2011), we were able to document the presence of sulfenylated MGL in intact Neuro-2a cells overexpressing the enzyme and exposed to H_2O_2 (300 μM) (Figure 2F). While we found no evidence of sulfenyl amide modification of C201 and C208, it is possible that this unstable chemical species was also transiently generated (Salmeen et al, 2003). Formation of a sulfenyl amide at C208 would explain why this residue is less prone to sulfenylation than is C201. Despite this unanswered question, the results outlined above clearly identify MGL residues C201 and C208 as targets for peroxide-dependent sulfenylation.

MGL sulfenylation interrupts 2-AG degradation in neurons

To determine whether cysteine sulfenylation influences 2-AG deactivation in intact cells, we incubated primary cultures of rat cortical neurons with H_2O_2 (30-300 μM) and measured

MGL activity in intact cells using a dedicated *in situ* assay. H_2O_2 inhibited MGL in a concentration-dependent manner (Figure 4A) and this effect was paralleled by an increase in intracellular 2-AG content (Figure 4B). By contrast, we observed no change in the levels of other lipids that are biogenetically or functionally related to 2-AG, including 1-steroyl-2-arachidonoyl-*sn*-glycerol (a 2-AG precursor), arachidonic acid (a product of 2-AG hydrolysis), or anandamide (an endocannabinoid neurotransmitter that is not hydrolyzed by MGL) (Figure 4C). The presence of sulfenylated MGL in H_2O_2-treated neurons was evaluated using affinity precipitation combined with western blot and LC/MS analyses. We incubated primary neurons in cultures with vehicle or H_2O_2 (300 μM), exposed them to the biotin-linked probe, BP1, and then concentrated sulfenyl-containing proteins by affinity precipitation using streptavidin-agarose beads. Blots probed with a selective anti-MGL antibody confirmed the presence of BP1-bound sulfenylated MGL in neurons exposed to H_2O_2, but not control neurons (Figure 4D). In a separate experiment, we subjected the affinity precipitates to shotgun LC-MS/MS proteomics. MGL peptides bearing BP1 bound to C201 (Figure 4E) or C208 (Figure 4F) were detected in precipitates of intact neurons treated with H_2O_2. Despite a low signal-to-noise ratio, due to the naturally low abundance of MGL, signals matching the predicted accurate mass values and charge states were detected in neurons treated with H_2O_2 (red traces), whereas no such signal was detected in control cells (black traces). Tandem MS data of the same peptides, matching the expected primary sequence, are reported in Figure S3. Additional evidence that the redox status can affect MGL activity was obtained by blocking glutathione (GSH) biosynthesis with the GSH synthase inhibitor, L-buthionine sulfoximine (BSO) (Griffith and Meister, 1979). Exposing cortical neurons to BSO depleted intracellular GSH stores (Figure 5A), lowered MGL activity (Figure 5B) and increased 2-AG content in a concentration-dependent (Figure 5C) and time-dependent manner (Figure S4). Confirming the generality of this response, experiments with cultures of mouse Neuro-2a cells yielded similar results (Figure S5).

MGL sulfenylation enhances 2-AG-mediated signaling

The data reported above suggest that MGL sulfenylation impairs 2-AG degradation, but does it also enhance 2-AG signaling? To address this question, we exploited the fact that CB_1 receptor activation protects neurons from oxidative damage (Nagayama et al, 1999; Panikashvili et al, 2001). We incubated Neuro-2a cells with a high concentration of H_2O_2 (300 μM) and assessed cell damage using three complementary methods: lactate dehydrogenase (LDH) release into the medium, 3-(4,5-dimethylthiazol-2-yl)-2,5-diphenyltetrazolium bromide (MTT) reduction and caspase-3 activity. In addition to native Neuro-2a cells, we assessed the effects of H_2O_2 on Neuro-2a cells overexpressing MGL (Figure 6) or the 2-AG-synthesizing enzyme DGL-α (Figure 7). As expected, MGL overexpression decreased cellular 2-AG levels, which were partially restored by treatment with the MGL inhibitor JZL184 (1 μM) (Figure 6A). Along with this effect, MGL overexpression enhanced H_2O_2-induced toxicity (Figure 6B-D), which was (a) heightened by the CB_1 antagonist rimonabant (but not by the CB_2 antagonist AM630) and (b) tempered by MGL blockade with JZL184 (Figure 6B-D). Conversely, DGL-α overexpression increased 2-AG levels in Neuro-2a cells (Figure 7A), and this response was accompanied by a substantial decrease in H_2O_2-induced toxicity (Figure 7B-D). The cytotoxic effect of H_2O_2 was reinstated by treatment with the CB_1 antagonist rimonabant (but not by the CB_2

antagonist AM630) (Figure 7B-D), suggesting that it was mediated by 2-AG-dependent activation of CB_1receptors. Consistent with this view, in primary neuronal cultures, H_2O_2 toxicity was enhanced by CB_1, but not CB_2, receptor blockade (Figure S6). Treatment with JZL184 alone did not affect cytotoxicity in Neuro-2a cells (LDH release %: vehicle control, 3.46 ± 0.59; JZL184, 1.73 ± 2.60, n=3). These observations indicate that peroxide-dependent MGL deactivation accrues the cellular pool of 2-AG that is involved in signaling at CB_1 receptors.

SIGNIFICANCE

Current models conceptualize 2-AG-dependent endocannabinoid transmission at excitatory synapses as being primarily, if not exclusively, driven by postsynaptic $mGluR_5$ activation and consequent 2-AG production (Castillo et al., 2012). Our findings expand this view by identifying sulfenylation-dependent MGL inhibition as a presynaptic mechanism through which the local redox state regulates 2-AG-mediated signaling. Physiopathological signals that stimulate H_2O_2 production might enhance the ability of 2-AG to modulate synaptic activity by temporarily interrupting 2-AG deactivation. The results also raise two questions. The first pertains to the sources of H_2O_2 involved in MGL regulation. Identifying such sources will require additional work, but likely candidates include mitochondria respiration (Sies, 2014) and ionotropic glutamate receptor-operated activation of NADPH oxidase (Brennan et al., 2009; Paulsen et al, 2011). The second question is connected to the first and concerns the context in which the redox control of MGL activity might be operational. Dysfunctional redox states such as brain ischemia are associated with rises in the levels of H_2O_2 and other reactive oxygen species (Armogida et al, 2012). In those conditions, MGL sulfenylation might act as an intrinsic neuroprotective mechanism by potentiating 2-AG signaling at CB_1 receptors. Nevertheless, localized foci of heightened H_2O_2 production (Mishina et al, 2011) might be sufficient to deactivate MGL even under physiological conditions, particularly at synapses that experience high-frequency synaptic activity and use glutamate as a neurotransmitter (Patel and Rice, 2012). In that context, MGL sulfenylation may strengthen endocannabinoid-mediated retrograde transmission by lowering the presynaptic degradation of 2-AG generated in postsynaptic spines. Activation of mitochondrial CB_1 receptors (Benard et al., 2012) might stimulate respiration and reactive oxygen species production, further enhancing this negative feedback loop. Finally, allosteric MGL modulators that exploit this regulatory process, such as benzisothiazolinone derivatives (King et al, 2009), might find therapeutic application in stroke, neurodegeneration and chronic neuropathic pain.

EXPERIMENTAL PROCEDURES

Materials

2-AG, 2-arachidonoyl-*sn*-glycerol-d_8 (2-AG-d_8), arachidonic acid-d_8 (AA-d_8), 4-nitrophenyl-4-(dibenzo[d][1,3]dioxol-5-yl(hydroxy)methyl)piperidine-1-carboxylate (JZL184) and [6-iodo-2-methyl-1-[2-(4-morpholinyl)ethyl]-1H-indol-3-yl](4-methoxyphenyl)-methanone (AM630) were purchased from Cayman Chemical (Ann Arbor, MI). 1,3-diheptadecanoyl-*sn*-glycerol (DHDG), 1(3)-heptadecenoyl-*sn*-glycerol (1-HG), 1(3)-oleoyl-*sn*-glycerol, heptadecanoic acid, and heptadecenoic acid were from Nu-Chek

Prep (Elysian, MN). BSO, dimethyl sulfoxide (DMSO), 2-oleoyl-*sn*-glycerol (2-OG), H_2O_2 and bovine serum albumin (BSA) were from Sigma-Aldrich (St. Louis, MO). *N*-(piperidin-1-yl)-5-(4-chlorophenyl)-1-(2,4-dichlorophenyl)-4-methyl-1*H*-pyrazole-3-carboximide hydrochloride (rimonabant) was from RTI International (Research Triangle Park, NC). Chromatography solvents were from Honeywell Burdick & Jackson (Muskegon, MI). Porcine trypsin (proteomic grade) was from Sigma Aldrich (Milan, Italy).

Enzyme assays

In vitro MGL activity was measured as described (King et al, 2007). Briefly, we transiently transfected HeLa cells with plasmid DNA encoding recombinant rat MGL using Superfect reagent (Qiagen, Valencia, CA). We harvested cells in ice-cold Tris-HCl (50 mM, pH 8.0) containing 0.32 M sucrose. We prepared homogenates by sonicating cells for 1 min on ice followed by 3 freeze-thawing cycles. Homogenates were incubated with various agents for 10 min at 37°C in assay buffer (50 mM Tris-HCl, pH 8.0 containing 0.5 mg/ml fatty acid-free BSA). The enzyme substrate 2-OG (10 μM), which we use in preference to 2-AG to increase signal-to-noise ratio in the assay, was added to the mixture and incubated for 10 additional min at 37°C. Reactions were stopped by adding chloroform:methanol (2:1, vol/vol), containing heptadecanoic acid (5 nmol/sample) as internal standard. After centrifugation at 2,000 × g at 4°C for 10 min, the organic layers were collected and dried under N_2. The lipid extracts were suspended in chloroform:methanol (1:3, vol/vol) and analyzed by liquid chromatography-mass spectrometry (LC-MS). Diacylglycerol lipase (DGL) activity was measured *in vitro* as described (Jung et al, 2007). Rapid dilution assays were performed as described (King et al, 2009; Copeland, 2005).

MGL activity assay *in situ*

MGL activity in primary cortical neurons was determined as described (Marrs et al, 2010) with minor modifications. Neurons were prepared using pregnant Wistar rats at embryonic day 18-20 (Stella and Piomelli, 2001). After 10 days in culture, cells were treated with the indicated reagents or vehicle for 30 min in B-27-supplemented Neurobasal medium (Life Technologies, Grand Island, NY). Cells were rinsed once with medium and incubated with substrate 1-HG (1 μM) for 10 min. After rinsing twice with ice-cold PBS, cells were harvested and lipids were extracted as described above, using heptadecanoic acid as internal standard. Non-specific hydrolysis of 1-HG was measured in the presence of excess 1(3)-oleoyl-*sn*-glycerol (100 μM), and baseline value was subtracted from each data point. Neuro-2a cells were partially differentiated by overnight serum deprivation and cultured in complete DMEM medium supplemented with 0.15% fatty acid free BSA.

Lipid quantitation

The levels of 2-AG, anandamide, arachidonic acid and 1-stearoyl-2-arachidonoyl-sn-glycerol (SAG) were determined by LC-MS or LC-MS/MS, as described (Jung et al, 2007).

Protein and western blot analyses

Bicinchoninic acid (BCA) protein assay and western blot analyses were performed as described (Jung et al, 2012) using monoclonal anti-V5 antibody (1:5,000, Life

Technologies), polyclonal anti-MGL antibody (1:1,000) (Dinh et al, 2002) and anti-actin monoclonal antibody (1:1,000, Calbiochem, La Jolla, CA).

Site-directed mutagenesis

Mutagenesis studies were performed using a QuikChange II XL Site-Directed Mutagenesis Kit (Strategene, La Jolla, CA) following manufacturer's instructions. We used rat MGL-pEF6/V5-His plasmid DNA as a template (King et al, 2009) and verified all plasmids by DNA sequencing.

MGL purification

Recombinant rat MGL was expressed in *E. coli* and purified as described (King et al, 2007) with minor modification.

Sulfenic acid trapping *in vitro*

A sample (200 μl) of MGL solution (40 μM) was transferred in a NanoSep 3K microcentrifuge tube (Pall Corporation, NY, USA) and buffer-exchanged (40×) versus HEPES (50 mM, pH 7.4), 300 mM NaCl 0.1% Triton X-100. The buffer was degassed with N_2 for 2 h prior to use. The sample was split into four 50-μl aliquots and incubated with dimedone at a final 20 mM concentration. H_2O_2 was added to final 0.1, 1 and 10 μM concentrations. Incubation without H_2O_2 was used as negative control. Only open-air oxidation was allowed for this control. The samples were incubated at 37°C for 1 h with shaking. Reactions were stopped adding 1 mL of cold acetone, and tubes were centrifuged at 14,000 rpm for 10 min. Acetone was removed and protein pellets were dried under N_2. The precipitate was further washed with 1 mL of methanol and then was dissolved in 50 μL of ammonium bicarbonate (50 mM, pH 8). Trypsin (1 μL of a 1 μg/μL solution) was added to each tube and samples were incubated at 37°C overnight. Samples were centrifuged at 10,000 × g for 10 min and diluted with 0.1% formic acid in water containing 1% acetonitrile for LC-MS analysis.

LC-MS/MS analyses of peptides

Tryptic peptides were separated using an Acquity UPLC BEH C18 (1 × 100 mm, 1.7 μm) column coupled to a Synapt G2 QTof mass spectrometer (Waters Inc. Milford, MA, USA). The following gradient conditions were used: A = 0.1% formic acid in water, B = 0.1% formic acid in acetonitrile. After 1 min at 97% A, a linear gradient was applied to 45% A in 12 min. then to 0%A in next 3 min, followed by 2 min at 0% A and reconditioning to 97% A in 0.1 min. Total run time was 19 min. Injection volume was set at 5 μL. MS and MS/MS analyses were performed in the positive ESI mode. The capillary voltages was set at 3 kV. The cone voltage was set at 30 V. The source temperature was 120°C. Desolvation gas and cone gas (N_2) flow were 600 and 20 L/h, respectively. Desolvation temperature was 400°C. Data were acquired in MSe mode with MS/MS fragmentation performed in the trap region. Low energy scans were acquired at fixed 4 eV potential and high energy scans were acquired with an energy ramp from 25 to 35 eV. Scan rate was set to 0.4 s per spectrum. Scan range was set to 50 to 1600 *m/z*. Leucine enkephalin (2 ng/ml) was infused as lock mass for spectra recalibration. LC-MS/MS data were analyzed using Proteinlynx software to

map MGL peptides, calculate MGL sequence coverage and quantify naïve and oxidized peptides. Additional de-novo sequencing of dimedone adducts at cysteine 201 and 208 was manually performed using Biolynx software to verify the peptide sequence and assign the modified residue.

Sulfenic acid trapping *in intact cells*

Neuro-2a cells were transfected with plasmids encoding MGL-V5 or the empty vector (pEF6) and, two days after transfection, were incubated with H_2O_2 for 1 h. Rat cortical neurons were treated with H_2O_2 for 1 h after 8 days *in vitro*. Following treatment, cells were scraped in lysis buffer containing 50 mM Tris-HCl, pH 7.4, 150 mM NaCl, 2 mM EDTA, 1% Triton X-100, and a mixture of protease inhibitors (Roche Diagnostics) in the presence or absence of 1 mM biotin-1,3-cyclopentanedione (BP1, KeraFAST, Boston, MA) (Qian et al, 2011). We incubated the mixtures on ice for 30 min with gentle mixing every 5 min. After centrifuging at 1,000 × g for 10 min at 4 °C, the supernatants were mixed with 10 μl of streptavidin-agarose (Pierce) at a protein concentration of 0.5 mg/ml, and incubated at 4°C overnight. The affinity precipitates were collected by brief centrifugation and washed 6 times with lysis buffer without BP1. For Western blot analyses, proteins in the precipitates were eluted by adding 20 μl of Laemmli sample buffer and incubating at 74°C for 20 min. For LC-MS/MS analyses, washed beads were stored in dry ice. Prior to LC-MS/MS, the beads were allowed to reach room temperature and were suspended in 25 ml of 2% SDS, 6 M urea and 2 M thiourea in PBS. Samples were kept 15 min at room temperature and then incubated at 96°C for 15 min to cleave the biotin-streptavidin bond (Rybak et al., 2004, with slight modifications). Samples were allowed to reach room temperature and were centrifuged for 10 min at 4000 × g. Supernatants were collected and the beads were further washed with 25 ml of water and incubated again at 96°C for 15 min. After centrifug ation (10 min, 4000 × g) the supernatants were pooled and the beads discarded. The resulting 50 ml of supernatant were added with 2 ml of 100 mM DTT and incubated at 50°C for 30 min. Iod oacetamide (100 mM, 4 ml) was added and the samples were incubated at room temperature for 30 min. After reduction and alkylation, released proteins were precipitated by adding 1 ml of ice-cold acetone and then centrifuged for 10 min at 4000 × g at 4°C. The supernatant was disc arded and the pellets were dried under N_2.

Samples were suspended in 40 ml Rapigest (Waters Inc.) previously dissolved in 100 mM ammonium bicarbonate, pH 8, at a final 1 mg/ml concentration. Trypsin was then added (1 ml, dissolved at 0.5 mg/ml in 0.1% formic acid) and the samples were incubated overnight at 37°C. The following day, samples were added with 1 ml of TFA, incubated at 37°C for 1 h and centrifuged to remove hydrolyzed Rapigest (10 min at 4000 × g). Supernatants were collected (30 ml) and added with 10 ml of formic acid 0.1% in water/acetonitrile (97:3). An aliquot (5 ml) was loaded on a nano-UPLC chromatographic system equipped with a T3 C18 reversed-phase column (75 mm × 250mm). Peptides were eluted with a linear gradient of acetonitrile in water (both containing 0.1% formic acid) from 3 to 50% in 120 min. Flow rate was set to 350 nl per min. Eluted peptides were analyzed in positive ion mode by high-resolution tandem mass spectrometry on a Synapt G2 qTOF mass spectrometer (Waters, Milford MA, USA). Tandem mass spectra were acquired in Data Dependent Acquisition mode (DDA), by selecting charge states ranging from 2 to 5 in the 300-1200 *m/z* range.

Collision energy was automatically set according to the precursor ion charge state and *m/z* value. MS and MS/MS spectra were recalibrated using glu-fibrinopeptide and leucine enkephalin respectively (both continuously infused in the source as Lock-Mass). Proteomics data were analyzed with both PLGS 3.2 and Biolynx softwares (Waters Inc.) to determine the presence and the primary sequence of the BP1 adducts of MGL peptides bearing C201 and C208.

Cell viability assays

Cell viability was assessed using the MTT assay, following a standard protocol (Sigma-Aldrich). Briefly, cells were seeded in 96-well plates at a concentration of 5×10^3 cells/well. After 24 h, they were transfected with MGL or DGL-α plasmids (0.5 μg DNA/well) and cultured for 24 h. They were treated with agents for 30 min, followed by a treatment with H_2O_2 (300 μM) for 24 h. MTT was added and plates were further incubated for 4 h. Absorbance was measured using a SpectraMax M5 microplate reader (Molecular Devices) at 570 nm with reference at 650 nm. Cell viability was calculated and expressed as percentage of control cells.

Cell death was quantified by measuring LDH release using a Cytotoxicity Detection Kit^{Plus} (Roche Diagnostics, Mannheim, Germany) and caspase-3 activation using a fluorescent assay kit (Cayman Chemical). Total GSH levels in cells were determined using an assay kit (Cayman Chemical).

Statistical analyses

All results are expressed as mean ± S.E.M. Non-linear regression analyses were performed using Prism version 5.0 (GraphPad Software Inc., La Jolla, CA). Statistical significance was assessed by two-tailed Student's *t* test or one-way ANOVA with Dunnett's post test.

Supplementary Material

Refer to Web version on PubMed Central for supplementary material.

ACKNOWLEDGEMENTS

This work was supported by grants DA012413 and DA031387 from NIDA (to D.P.). The contribution of the Agilent Technologies/University of California, Irvine Analytical Discovery Facility, is gratefully acknowledged.

REFERENCES

Armogida M, Nisticò R, Mercuri NB. Therapeutic potential of targeting hydrogen peroxide metabolism in the treatment of brain ischaemia. Br. J. Pharmacol. 2012; 166:1211–1124. [PubMed: 22352897]

Bénard G, Massa F, Puente N, Lourenço J, Bellocchio L, Soria-Gómez E, Matias I, Delamarre A, Metna-Laurent M, Cannich A, Hebert-Chatelain E, Mulle C, Ortega-Gutiérrez S, Martín-Fontecha M, Klugmann M, Guggenhuber S, Lutz B, Gertsch J, Chaouloff F, López-Rodríguez ML, Grandes P, Rossignol R, Marsicano G. Mitochondrial CB_1 receptors regulate neuronal energy metabolism. Nat Neurosci. 2012; 15:558–564. [PubMed: 22388959]

Bertrand T, Augé F, Houtmann J, Rak A, Vallée F, Mikol V, Berne PF, Michot N, Cheuret D, Hoornaert C, Mathieu M. Structural basis for human monoglyceride lipase inhibition. J. Mol. Biol. 2010; 396:663–673. [PubMed: 19962385]

Brennan AM, Suh SW, Won SJ, Narasimhan P, Kauppinen TM, Lee H, Edling Y, Chan PH, Swanson RA. NADPH oxidase is the primary source of superoxide induced by NMDA receptor activation. Nat. Neurosci. 2009; 12:857–863. [PubMed: 19503084]

Castillo PE, Younts TJ, Chávez AE, Hashimotodani Y. Endocannabinoid signaling and synaptic function. Neuron. 2012; 76:70–81. [PubMed: 23040807]

Copeland RA. Evaluation of enzyme inhibitors in drug discovery. A guide for medicinal chemists and pharmacologists. Methods Biochem. Anal. 2005; 46:1–265. [PubMed: 16350889]

Denu JM, Tanner KG. Specific and reversible inactivation of protein tyrosine phosphatases by hydrogen peroxide: evidence for a sulfenic acid intermediate and implications for redox regulation. Biochemistry. 1998; 37:5633–5642. [PubMed: 9548949]

Dickinson BC, Chang CJ. Chemistry and biology of reactive oxygen species in signaling or stress responses. Nat. Chem. Biol. 2011; 7:504–511. [PubMed: 21769097]

Dinh TP, Carpenter D, Leslie FM, Freund TF, Katona I, Sensi SL, Kathuria S, Piomelli D. Brain monoglyceride lipase participating in endocannabinoid inactivation. Proc. Natl. Acad. Sci. U S A. 2002; 99:10819–10824. [PubMed: 12136125]

Griffith OW, Meister A. Potent and specific inhibition of glutathione synthesis by buthionine sulfoximine (S-n-butyl homocysteine sulfoximine). J. Biol. Chem. 1979; 254:7558–7560. [PubMed: 38242]

Gulyas AI, Cravatt BF, Bracey MH, Dinh TP, Piomelli D, Boscia F, Freund TF. Eur. J. Neurosci. 2004; 20:441–458. [PubMed: 15233753]

Hohmann AG, Suplita RL, Bolton NM, Neely MH, Fegley D, Mangieri R, Krey JF, Walker JM, Holmes PV, Crystal JD, Duranti A, Tontini A, Mor M, Tarzia G, Piomelli D. An endocannabinoid mechanism for stress-induced analgesia. Nature. 2005; 435:1108–1112. [PubMed: 15973410]

Jung KM, Clapper JR, Fu J, D'Agostino G, Guijarro A, Thongkham D, Avanesian A, Astarita G, DiPatrizio NV, Frontini A, Cinti S, Diano S, Piomelli D. 2-arachidonoylglycerol signaling in forebrain regulates systemic energy metabolism. Cell Metab. 2012; 15:299–310. [PubMed: 22405068]

Jung KM, Astarita G, Zhu C, Wallace M, Mackie K, Piomelli D. A key role for diacylglycerol lipase-alpha in metabotropic glutamate receptor-dependent endocannabinoid mobilization. Mol. Pharmacol. 2007; 72:612–621. [PubMed: 17584991]

Katona I, Freund TF. Endocannabinoid signaling as a synaptic circuit breaker in neurological disease. Nat. Med. 2008; 14:923–930. [PubMed: 18776886]

King AR, Dotsey EY, Lodola A, Jung KM, Ghomian A, Qiu Y, Fu J, Mor M, Piomelli D. Discovery of potent and reversible monoacylglycerol lipase inhibitors. Chem. Biol. 2009; 16:1045–1052. [PubMed: 19875078]

King AR, Duranti A, Tontini A, Rivara S, Rosengarth A, Clapper JR, Astarita G, Geaga JA, Luecke H, Mor M, Tarzia G, Piomelli D. URB602 inhibits monoacylglycerol lipase and selectively blocks 2-arachidonoylglycerol degradation in intact brain slices. Chem. Biol. 2007; 14:1357–1365. [PubMed: 18096504]

Labar G, Bauvois C, Borel F, Ferrer JL, Wouters J, Lambert DM. Crystal structure of the human monoacylglycerol lipase, a key actor in endocannabinoid signaling. Chembiochem. 2010; 11:218–227. [PubMed: 19957260]

Lo Conte M, Carroll KS. The redox biochemistry of protein sulfenylation and sulfinylation. J. Biol. Chem. 2013; 288:26480–26488. [PubMed: 23861405]

Long JZ, Li W, Booker L, Burston JJ, Kinsey SG, Schlosburg JE, Pavón FJ, Serrano AM, Selley DE, Parsons LH, Lichtman AH, Cravatt BF. Selective blockade of 2-arachidonoylglycerol hydrolysis produces cannabinoid behavioral effects. Nat. Chem. Biol. 2009; 5:37–44. [PubMed: 19029917]

Marrs WR, Blankman JL, Horne EA, Thomazeau A, Lin YH, Coy J, Bodor AL, Muccioli GG, Hu SS, Woodruff G, Fung S, Lafourcade M, Alexander JP, Long JZ, Li W, Xu C, Möller T, Mackie K, Manzoni OJ, Cravatt BF, Stella N. The serine hydrolase ABHD6 controls the accumulation and efficacy of 2-AG at cannabinoid receptors. Nat. Neurosci. 2010; 13:951–957. [PubMed: 20657592]

Mishina NM, Tyurin-Kuzmin PA, Markvicheva KN, Vorotnikov AV, Tkachuk VA, Laketa V, Schultz C, Lukyanov S, Belousov VV. Does cellular hydrogen peroxide diffuse or act locally? Antioxid. Redox Signal. 2011; 14:1–7. [PubMed: 20690882]

Nagayama T, Sinor AD, Simon RP, Chen J, Graham SH, Jin K, Greenberg DA. Cannabinoids and neuroprotection in global and focal cerebral ischemia and in neuronal cultures. J. Neurosci. 1999; 19:2987–2995. [PubMed: 10191316]

Pan J, Carroll KS. Chemical biology approaches to study protein cysteine sulfenylation. Biopolymers. 2014; 101:165–172. [PubMed: 23576224]

Panikashvili D, Simeonidou C, Ben-Shabat S, Hanus L, Breuer A, Mechoulam R, Shohami E. An endogenous cannabinoid (2-AG) is neuroprotective after brain injury. Nature. 2001; 413:527–531. [PubMed: 11586361]

Patel JC, Rice ME. Classification of H_2O_2 as a neuromodulator that regulates striatal dopamine release on a subsecond time scale. ACS Chem. Neurosci. 2012; 3:991–1001. [PubMed: 23259034]

Paulsen CE, Truong TH, Garcia FJ, Homann A, Gupta V, Leonard SE, Carroll KS. Peroxide-dependent sulfenylation of the EGFR catalytic site enhances kinase activity. Nat. Chem. Biol. 2011; 8:57–64. [PubMed: 22158416]

Qian J, Klomsiri C, Wright MW, King SB, Tsang AW, Poole LB, Furdui CM. Simple synthesis of 1,3-cyclopentanedione derived probes for labeling sulfenic acid proteins. Chem. Commun. (Camb). 2011; 47:9203–9205. [PubMed: 21738918]

Rice ME. H_2O_2: a dynamic neuromodulator. Neuroscientist. 2011; 17:389–406. [PubMed: 21666063]

Rybak JN, Scheurer SB, Neri D, Elia G. Purification of biotinylated proteins on streptavidin resin: a protocol for quantitative elution. Proteomics. 2004; 4:2296–2299. [PubMed: 15274123]

Saario SM, Salo OM, Nevalainen T, Poso A, Laitinen JT, Järvinen T, Niemi R. Characterization of the sulfhydryl-sensitive site in the enzyme responsible for hydrolysis of 2-arachidonoyl-glycerol in rat cerebellar membranes. Chem. Biol. 2005; 12:649–656. [PubMed: 15975510]

Salmeen A, Andersen JN, Myers MP, Meng TC, Hinks JA, Tonks NK, Barford D. Redox regulation of protein tyrosine phosphatase 1B involves a sulphenyl-amide intermediate. Nature. 2003; 423:769–773. [PubMed: 12802338]

Schalk-Hihi C, Schubert C, Alexander R, Bayoumy S, Clemente JC, Deckman I, DesJarlais RL, Dzordzorme KC, Flores CM, Grasberger B, Kranz JK, Lewandowski F, Liu L, Ma H, Maguire D, Macielag MJ, McDonnell ME, Mezzasalma Haarlander T, Miller R, Milligan C, Reynolds C, Kuo LC. Crystal structure of a soluble form of human monoglyceride lipase in complex with an inhibitor at 1.35 Å resolution. Protein Sci. 2011; 20:670–683. [PubMed: 21308848]

Sies H. Role of metabolic H2O2 generation: redox signaling and oxidative stress. J. Biol. Chem. 2014; 289:8735–8741. [PubMed: 24515117]

Stella N, Piomelli D. Receptor-dependent formation of endogenous cannabinoids in cortical neurons. Eur. J. Pharmacol. 2001; 425:189–196. [PubMed: 11513837]

Highlights

- The second messenger hydrogen peroxide inhibits monoacylglycerol lipase (MGL)
- Hydrogen peroxide sulfenylates cysteines C201 and C208 in MGL
- MGL sulfenylation elevates 2-AG-mediated endocannabinoid signaling in neurons
- MGL oxidation may serve a presynaptic control point for endocannabinoid signaling

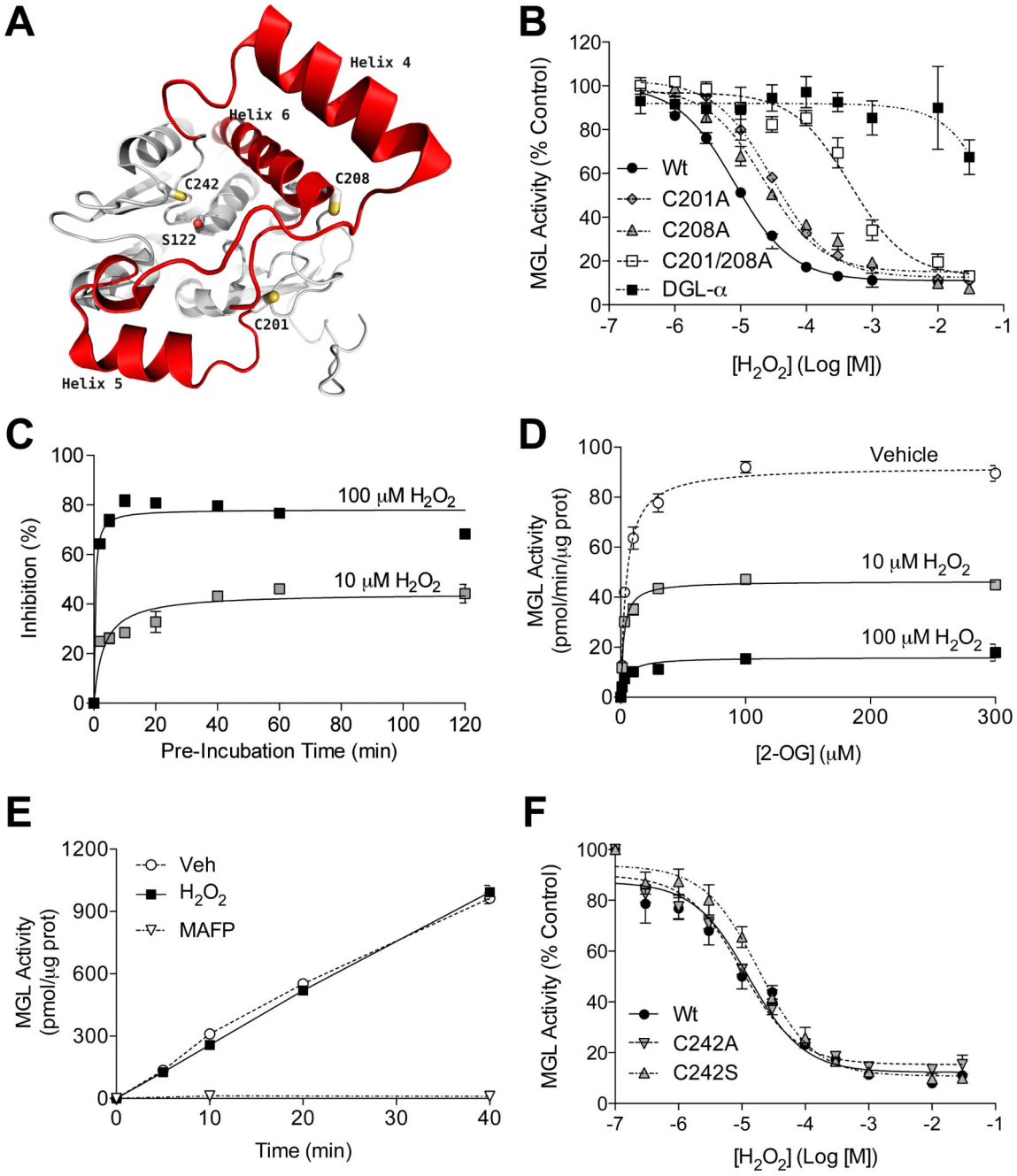

Figure 1. Hydrogen peroxide inhibits MGL

(**A**) Structure of human MGL showing cysteine residues C201 and C208 (on the cap domain, red) and C242 (close to catalytic nucleophile S122). (**B**) Effects of H_2O_2 on wild-type MGL (filled circles), MGL mutants C201A (filled diamonds), C208A (filled triangles) or C201/208A (empty squares) and DGL-α (filled squares). (**C**) Time-course of MGL inhibition by H_2O_2 (10 μM: shaded squares; 100 μM: filled squares). (**D**) Kinetics of MGL inhibition by H_2O_2 (vehicle: open circles). (**E**) Rapid dilution of MGL incubated with vehicle (circles), H_2O_2 (filled squares; 10 μM final), or irreversible inhibitor

methylarachidonylfluorophosphonate (MAFP, inverted triangles, 23 nM final). (**F**) Effects of H_2O_2 on wild-type MGL (filled circles) and MGL C242 mutants C242A (inverted triangles) and C242S (triangles).

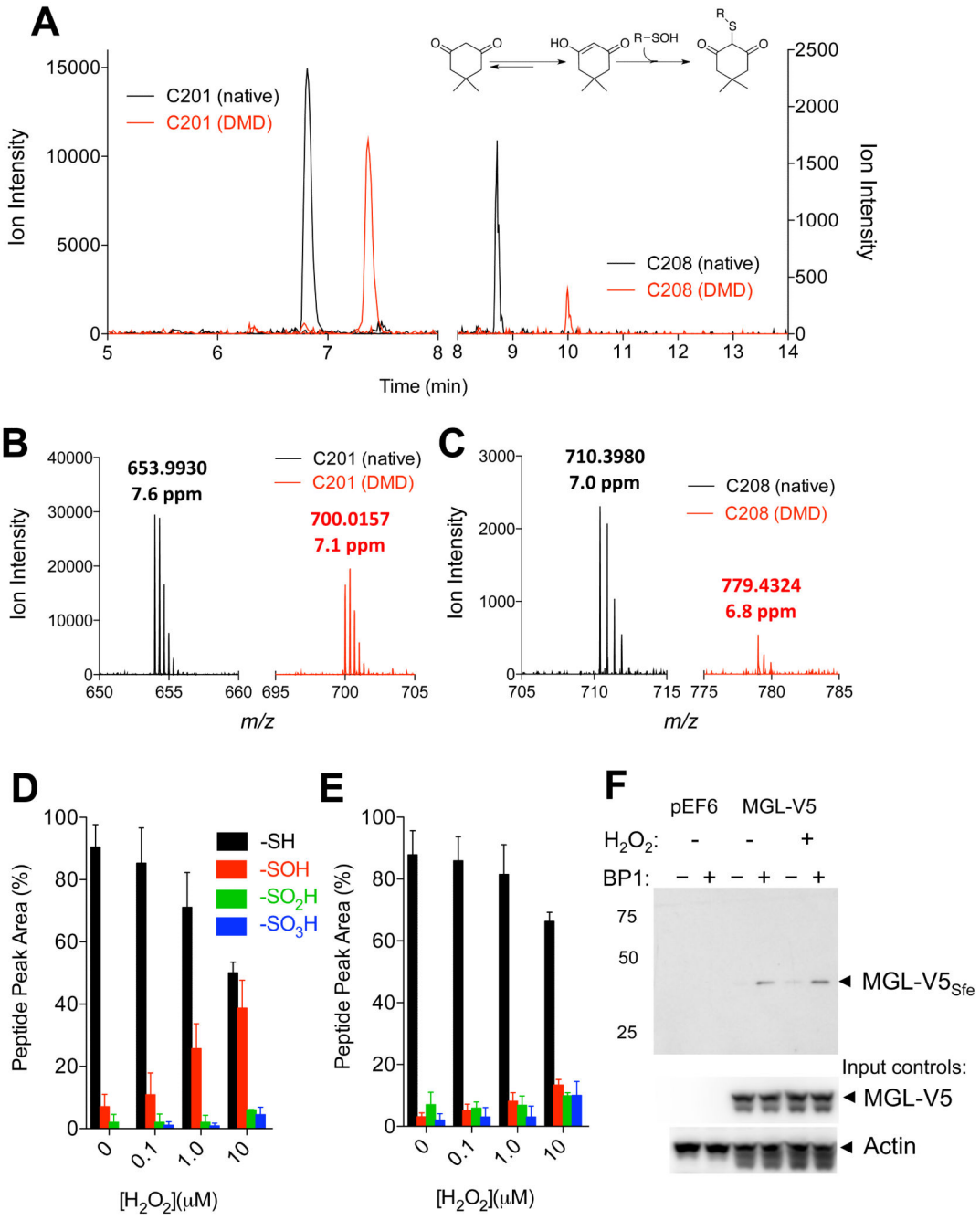

Figure 2. Hydrogen peroxide sulfenylates MGL

(**A**) Extracted-ion currents of native (black) and dimedone (DMD)-containing (red) peptides obtained by digestion of rat MGL exposed to H_2O_2 (10 μM, 1h). Inset: reaction of DMD with sulfenylated cysteine. (**B,C**) Mass spectra regions showing that DMD binds to C201 (**B**) and C208 (**C**). The observed *m/z* values and the corresponding mass errors are listed above the peaks. (**D,E**) Relative abundance of C201 and C208 present as native (-SH), sulfenic (-SOH, dimedone adduct), sulfinic ($-SO_2H$) and sulfonic acid ($-SO_3H$) at varying H_2O_2 concentrations. (**F**) Detection of sulfenylated MGL (MGL-$V5_{Sfe}$) in Neuro-2a cells

after H_2O_2 treatment (100 μM, 1h). Sulfenylated MGL was trapped using the chemoselective probe biotin-1,3-cyclopentanedione (BP1). Equal sample loading to the affinity precipitation was confirmed by assessing levels of MGL (using an anti-V5 antibody) and actin (input controls). 75, 50, 25: molecular weight size markers (kDa).

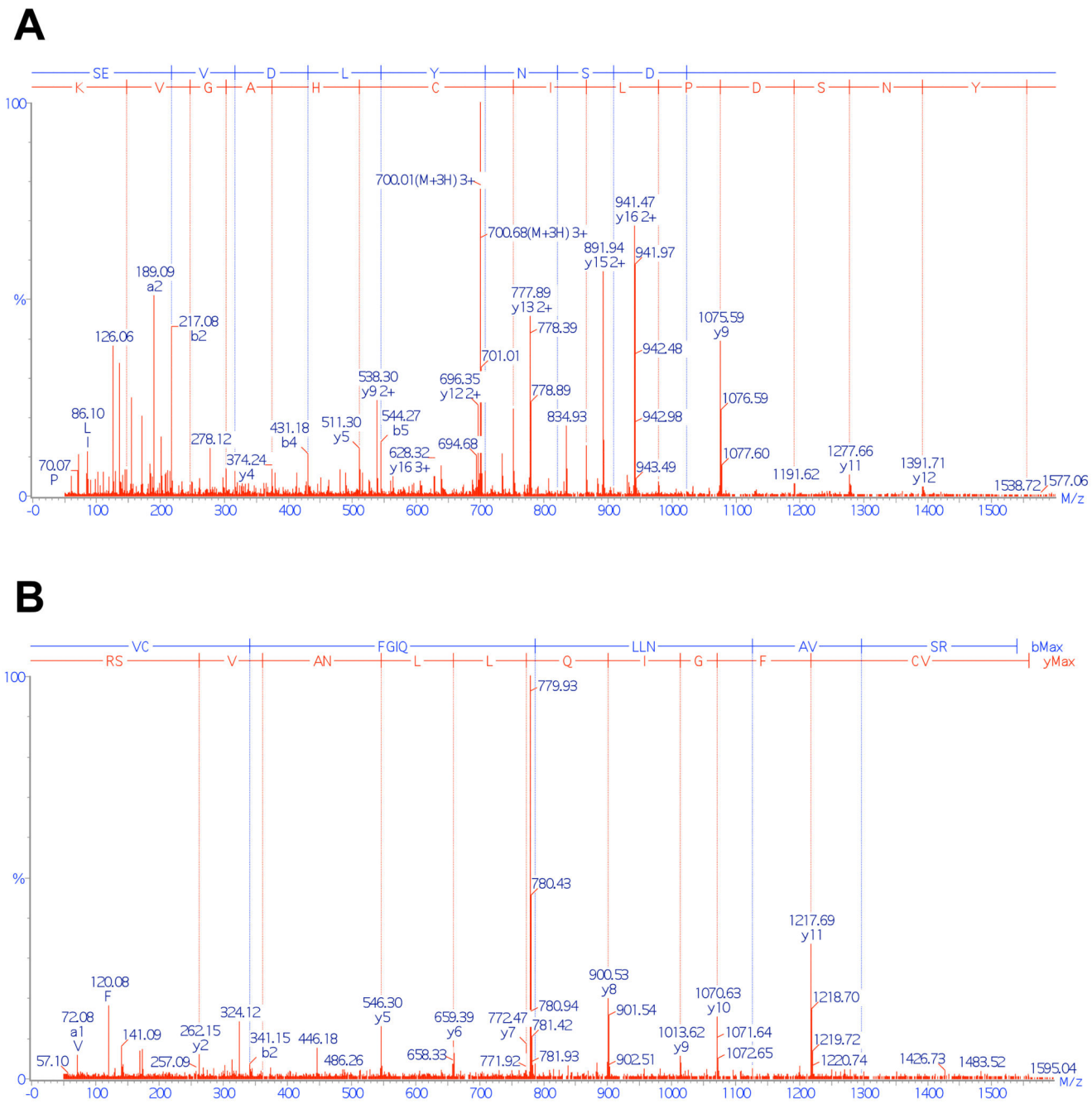

Figure 3. Tandem mass analyses of cysteine-containing tryptic fragments of MGL treated with hydrogen peroxide

(**A**) Tandem mass spectra of peptide SEVDLYNSDPLI**C**HAGVK, showing that sulfenylation (detected as DMD adduct) occurred on C201. (**B**) Tandem mass spectra of peptide V**C**FGIQLLNAVSR, showing that sulfenylation (detected as DMD adduct) occurred on C208.

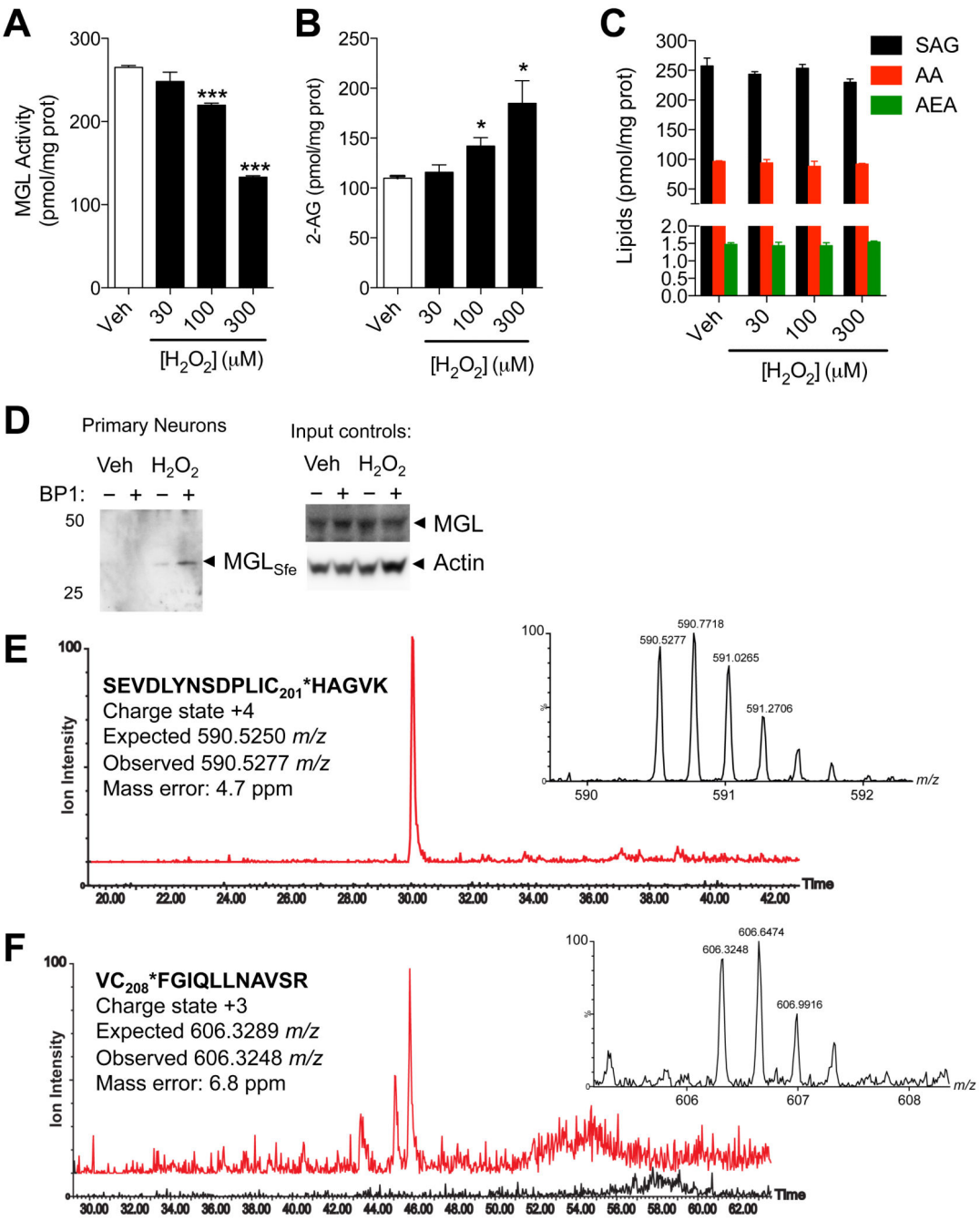

Figure 4. Peroxide-dependent inhibition of MGL activity and 2-AG accumulation in brain neurons

(**A-D**) Effects of H_2O_2 (filled bars) or vehicle (open bars) on (**A**) MGL activity, (**B**) 2-AG levels, and (**C**) 1-stearoyl,2-arachidonoylglycerol (SAG), arachidonic acid (AA), and anandamide (AEA) in rat cortical neurons in primary cultures. (**D**) Detection of sulfenylated MGL (MGL_{Sfe}) in primary cortical neurons in cultures after H_2O_2 treatment (300 μM, 1h). Sulfenylated MGL was trapped using the chemoselective probe BP1. Equal sample loading to the affinity precipitation was confirmed by measuring MGL (anti-MGL antibody) and

actin (input controls). 50, 25: molecular weight size markers (kDa). (**E**) Ion current of the BP1-adduct of MGL peptide bearing C201 (590.53 *m/z*, z=4) extracted from the control incubation (black trace) and incubation of neurons with H_2O_2 (red trace). (**F**) Ion current of the BP1-adduct of MGL peptide bearing C208 (606.30 *m/z*, z=3) extracted from the control incubation (black trace) and incubation of neurons with H_2O_2 (red trace). In both **E** and **F**, the high-resolution mass spectra reported in the inset matches the expected charge state and *m/z* value. ***$P<0.001$ and *$P<0.05$ compared to vehicle, two-tailed Student's *t* test.

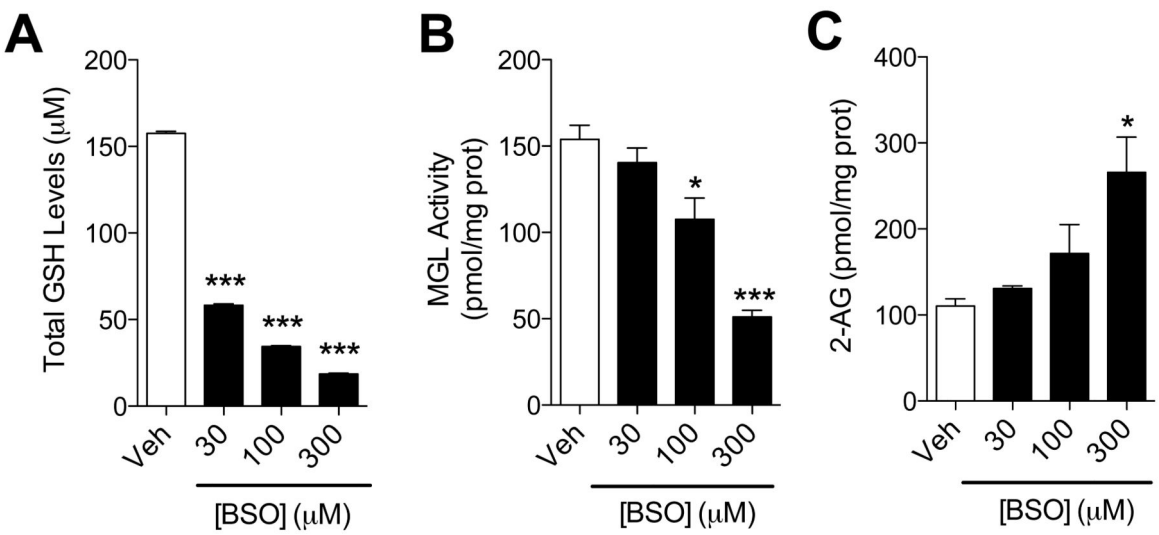

Figure 5. GSH depletion inhibits MGL activity and causes 2-AG accumulation in brain neurons

(**A**-**C**) Effects of BSO (filled bars) or vehicle (open bars) on (**A**) GSH levels, (**B**) MGL activity and (**C**) 2-AG levels in neuronal cultures. ***$P<0.001$ and *$P<0.05$ compared to vehicle, two-tailed Student's *t* test.

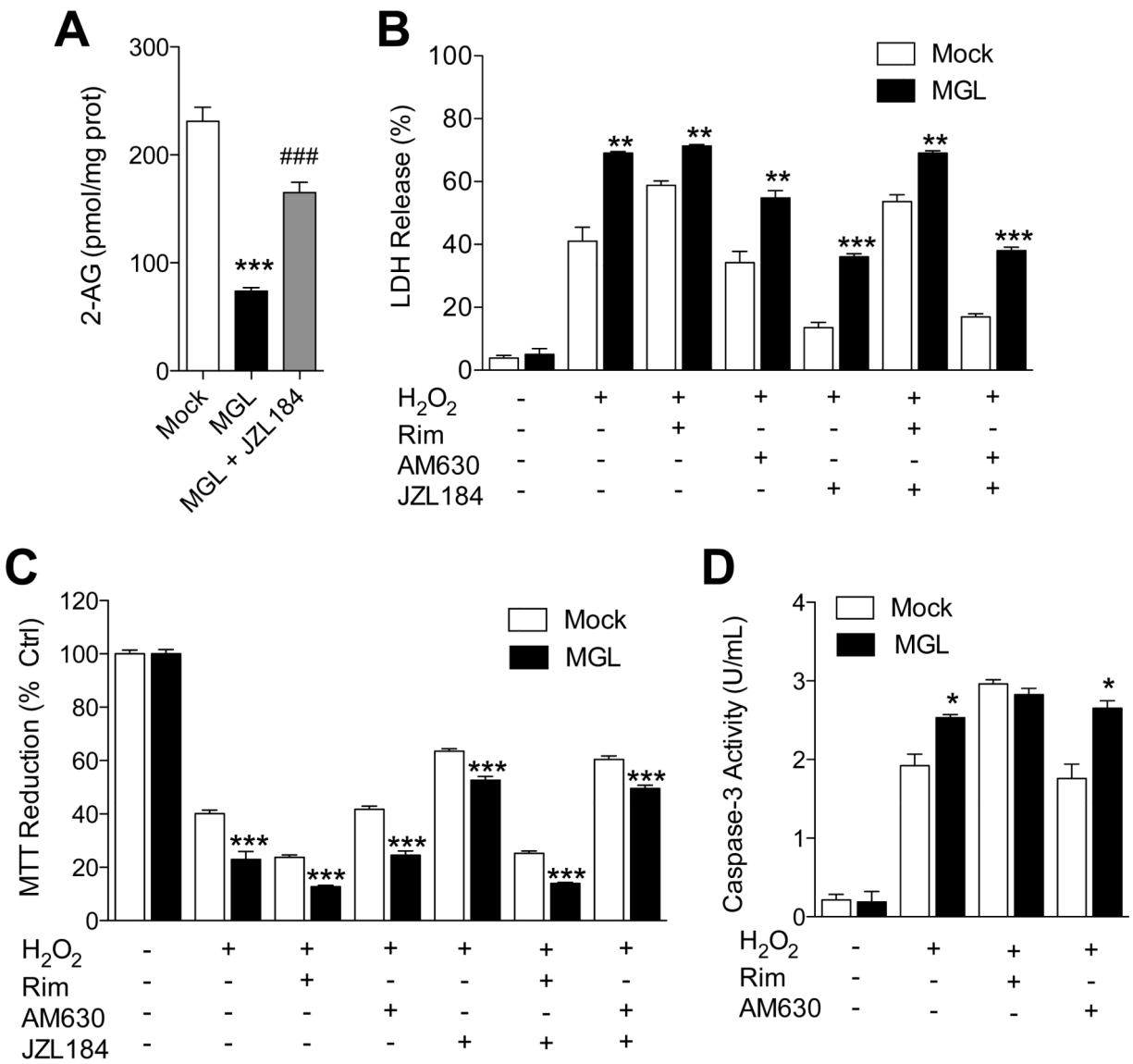

Figure 6. Reduction of 2-AG levels attenuates peroxide-dependent CB_1 signaling

(**A**) 2-AG levels in Neuro-2a cells overexpressing MGL. (**B-D**) Effects of H_2O_2, alone or combined with CB_1 antagonist rimonabant, CB_2 antagonist AM630 or MGL inhibitor JZL184 (each at 1 μM), on wild-type (open bars) or MGL-overexpressing Neuro-2a cells: (**B**) LDH release, (**C**) MTT reduction, and (**D**) caspase-3 activity. ***P<0.001, **P<0.05 and * P<0.05 compared to Mock, and $^{###}P$<0.001 compared to MGL, two-tailed Student's t test.

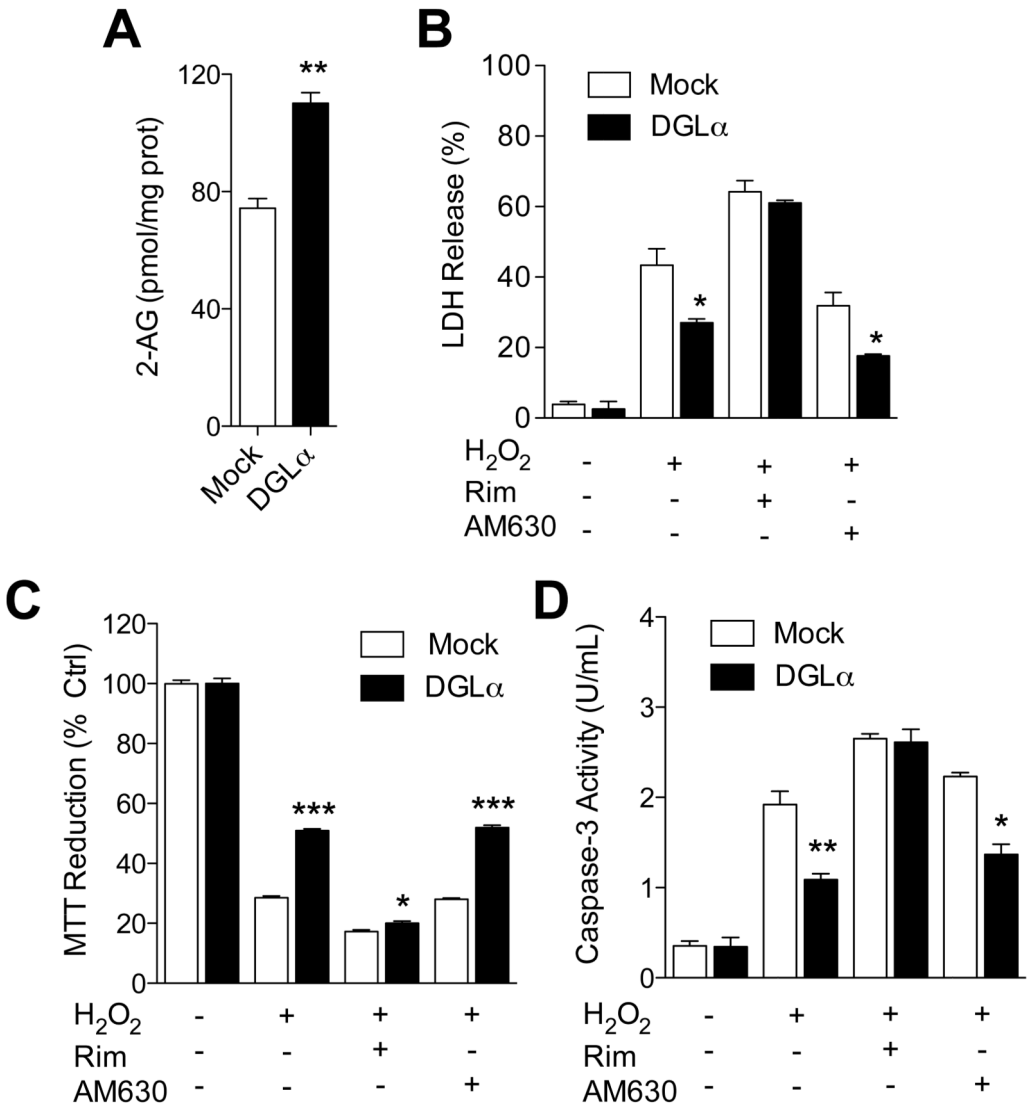

Figure 7. Elevation of 2-AG levels strengthens peroxide-dependent CB_1 signaling

(**A**) 2-AG levels in Neuro-2a cells overexpressing DGL-α. (**B-D**) Effects of H_2O_2, alone or combined with rimonabant, AM630 or JZL184, on wild-type or DGL-α–overexpressing Neuro-2a cells: (**B**) LDH release, (**C**) MTT reduction, and (**D**) caspase-3 activity. ***P<0.001, **P<0.05 and * P<0.05 compared to Mock, two-tailed Student's t test.